arXiv:1612.01405v1 [cond-mat.soft] 2 Dec 2016

Heterogeneous dynamics during yielding of glasses: effect of aging

Gaurav Prakash Shrivastav,[1] Pinaki Chaudhuri,[2] and Jürgen Horbach[1]

[1)] *Institut für Theoretische Physik II, Heinrich-Heine-Universität Düsseldorf, Universitätsstr. 1, 40225 Düsseldorf, Germany*

[2)] *The Institute of Mathematical Sciences, CIT Campus, Taramani, Chennai 600 113, India*

Molecular dynamics computer simulations of a binary Lennard-Jones glass under shear are presented. The mechanical response of glassy states having different thermal histories is investigated by imposing a wide range of external shear rates, at different temperatures. The stress-strain relations exhibit an overshoot at a strain of around 0.1, marking the yielding of the glass sample and the onset of plastic flow. The amplitude of the overshoot shows a logarithmic behavior with respect to a dimensionless variable, given by the age of the sample times the shear rate. Dynamical heterogeneities having finite lifetimes, in the form of shear bands, are observed as the glass deforms under shear. By quantifying the spatial fluctuations of particle mobility, we demonstrate that such shearbanding occurs only under specific combinations of imposed shear-rate, age of glass and ambient temperature.

I. INTRODUCTION

The mechanical properties of amorphous solids have been harnessed extensively in designing materials which are ubiquitous in our everyday life. However, a complete microscopic understanding of the mechanisms leading to the macroscopic response of these materials is still missing. In order to develop materials with specific functions, it is necessary to have an improved knowledge of these underlying processes. This remains a challenging task.

It is known that the material properties of amorphous solids, such as colloidal or metallic glasses, depend on their history of production, e.g. the cooling rate by which they were quenched from a fluid phase[1]. This dependence on the history, i.e. the age of the amorphous solid, is an important issue in computer simulations of glasses, especially because the accessible cooling rates in simulations are many orders of magnitudes larger than those accessible in experiments of real systems. With respect to the comparison between simulation and experiment, it is therefore crucial to systematically understand the dependence of structural and dynamic properties on the age of the glassy solid.

It is thus expected that the response of a glass to an external mechanical loading is affected by the age of the glass. If one shears an amorphous solid under a constant strain rate, it is in general transformed into a flowing fluid[2,3]. While at sufficiently high strains, the flowing fluid reaches a steady state without any memory of the initial unsheared state, the transient response to the shear is affected by the history of the initial glass state. The characteristic stress-strain relation of a glassy system, in response to an externally applied shear rate, exhibits typically a maximum at a strain of the order of 0.1[4]. In numerical simulations of sheared thermal glasses, the amplitude of this maximum is observed to depend on the age of the material, typically growing logarithmically with increasing age[5,6].

Moreover, the transient response of glasses to an external shear field is often associated with the occurrence of shear bands, i.e. band-like structures with strain or mobility higher than other regions, observed both in experiments[7–14] and numerical simulations[15–22]. Such spatially localised structures are seen to emerge after the occurrence of the stress overshoot, as the stress relaxes to the steady state value. Also, the formation of these transient shearbands have been observed to be influenced by the thermal history of the glassy state, with states which are obtained by faster cooling being less susceptible to shearband formation. Further, it has been noted that such a spatially heterogeneous response is more likely to

occur in the transient regime beyond the stress overshoot, at any given temperature.

The focus of our study are thermal glasses which are often characterized as simple yield stress fluids, e.g. colloids, emulsions. For such materials, the steady state flow curve (i.e. stress vs. imposed shear rate) is a monotonic function[12,23,24].. Thus there are no persistent shear-bands, which would be the case for non-monotonic flow curves[10,17,25,26]. In the case of simple yield stress fluids, the transient shearband that emerges are seen to broaden with time and eventually the entire material is fluidized, with the timescale of fluidization depending on the imposed shear-rate or stress[14,16,27]. Such spatio-temporal fluctuations are also visible during steady flow, both in experiments and simulations[12,15,28]. However, in this work, our objective is to characterize the transient spatial heterogeneities, prior to onset of steady flow.

The formation of transient shearbands has been addressed within the scope of various theoretical models. Within the framework of spatially-resolved fluidity and soft-glass-rheology (SGR) models[10,29,30], the age-dependent spatially heterogeneous response has been obtained, with the occurrence of the stress-overshoot under an applied shear-rate being associated with an instability leading to the formation of these transient heterogeneities. The model recovers the observation that more pronounced and long-lived shearbanding occurs for more aged glassy samples. Similarly, Manning et al.[31,32] also observe various transient heterogeneous states, by analysing a shear-transformation-zone (STZ) model of glassy materials, which depend upon the initial state of the system (characterised by an initial effective temperature) and the imposed shear-rate. Further, they were able to map their results to those obtained from numerical simulations[33]. The same phenemenology has also been reproduced by other mesoscopic models[34,35].

In this work, we address the question how the combination of ambient temperature, applied shear-rate and age of the glass affects the transient response, specifically the observation of spatio-temporal heterogeneities. This has not been systematically studied in earlier numerical simulations. Consequently, we also compare our observations with those from the theoretical models.

To this end, we perform molecular dynamics computer simulations of the Kob-Andersen binary Lennard-Jones (KABLJ) model[36], a well-studied glass former. Amorphous states are prepared by quenching a supercooled liquid to different temperatures below the mode coupling temperature, followed by a relaxation of the sample over a waiting time t_{w}. Then,

the resulting glass samples are sheared with different shear rates $\dot{\gamma}$. The onset of plastic flow occurs around the location of $\sigma^{\max}$, i.e. at a strain $\gamma^{\max} = \dot{\gamma}t^{\star} \approx 0.1$ (with $t^{\star}$ the time at which the maximum is obtained), with the appearance of a peak in the stress-strain response. We demonstrate that at the different temperatures T, the peak height, $\sigma_{\max}$, for all ages and shear-rates, obeys the functional behavior $C(\dot{\gamma}, T) + A(T)\ln(\dot{\gamma}t_{\rm w})$ (with C a function depending on $\dot{\gamma}$ and T and A a temperature-dependent amplitude). Note that this finding is consistent with earlier studies[5,6]. Further, as we have shown recently[18], transient (but long-lived) shear bands are formed for $\gamma > \gamma^{\max}$, provided that shear rate is sufficiently low. We quantify the contrast in spatial mobilities and demonstrate that the extent of spatial heterogeneities is not only dependent on the age of the glass, but also on the ambient temperature.

The rest of the paper is organized as follows. In Sec. II we describe the KABLJ model and the details of the simulation. Then, we present the results for the stress-strain relations and the analysis in terms of mobility maps in Sec. III. Finally, in Sec. IV, we summarize the results and draw some conclusions.

II. MODEL AND METHODS

We consider a binary mixture of Lennard-Jones (LJ) particles (say A and B) with 80:20 ratio. This is a well-studied glass former. Particles interact via LJ potential which is defined as:

$$\begin{aligned} \mathrm{U}^{\rm LJ}_{\alpha\beta}(r) &= \phi_{\alpha\beta}(r) - \phi_{\alpha\beta}(R_c) - (r - R_c)\left.\frac{d\phi_{\alpha\beta}}{dr}\right|_{r=R_c}, \\ \phi_{\alpha\beta}(r) &= 4\epsilon_{\alpha\beta}\left[(\sigma_{\alpha\beta}/r)^{12} - (\sigma_{\alpha\beta}/r)^{6}\right] \; r < R_c, \end{aligned} \tag{1}$$

where α, β = A, B. The interaction parameters are given by $\epsilon_{\rm AA} = 1.0$, $\epsilon_{\rm AB} = 1.5\epsilon_{\rm AA}$, $\epsilon_{\rm BB} = 0.5\epsilon_{\rm AA}$, $\sigma_{\rm AA} = 1.0$, $\sigma_{\rm AB} = 0.8\sigma_{\rm AA}$, $\sigma_{\rm BB} = 0.88\sigma_{\rm AA}$, and $R_c = 2.5\sigma_{\rm AA}$. Masses of both type of particles are equal, i.e., $m_{\rm A} = m_{\rm B} = m$. All quantities are expressed in LJ units in which the unit of length is $\sigma_{\rm AA}$, energy is expressed in the units of $\epsilon_{\rm AA}$ and the unit of time is $\sqrt{m\sigma^2_{\rm AA}/\epsilon_{\rm AA}}$. More details about the model and parameters can be found in Ref.[36].

We perform molecular dynamics (MD) simulation in the NVT ensemble using the package LAMMPS ("Large-scale Atomic/Molecular Massively Parallel Simulator")[37]. The simulations are done for the box geometry having the dimension $20 \times 20 \times 80$. Temperature is kept

constant via a dissipative particle dynamics (DPD) thermostat[38].

Our method for the preparation of the glass samples is as follows: At a density $\rho = 1.2$, we first equilibrate the system at the temperature $T = 0.45$, which is in the super-cooled regime. Then, we quench it to the target temperatures $T = 0.2, 0.3, 0.4$, below the mode coupling transition temperature[36]. For exploring the effect of aging on the mechanical response, we sample glassy states having different ages, $t_{\rm w} = 10^2, 10^3, 3 \times 10^3, 10^4, 3 \times 10^4$ and 10^5, as the system evolves after the quench to each target temperature. Using these initial states sampled at different $t_{\rm w}$, we apply shear on x-z plane in the direction of x with different constant strain rates $\dot{\gamma} = 10^{-2}, 10^{-3}, 3 \times 10^{-4}, 10^{-4}, 3 \times 10^{-5}$ and 10^{-5}. To simulate a bulk glass under shear, we use Lees-Edwards periodic boundary conditions[39].

III. RESULTS

In order to characterize the mechanical response of the aged amorphous solids, we measured different structural and dynamical properties, both at the macroscopic and local scales. We now discuss these observation in detail.

A. Macroscopic response

1. Stress vs strain

When the externally applied shear is imposed on the aging quiescent glass, the deformation response of the material is characterized by measuring the stress, $\sigma_{\rm xz}$, generated in the system with increasing strain ($\dot{\gamma}t$). In Fig. 1(a), we show how the stress evolves when we impose $\dot{\gamma} = 10^{-4}$ on initial states sampled from different ages, at $T = 0.2$. We observe the characteristic stress overshoot[5], with the peak height ($\sigma^{\rm max}$) increasing for larger $t_{\rm w}$. Across temperatures, within the glassy regime, this characteristic response does not change. However, as expected the material becomes less rigid with increasing temperature. For example, for a fixed age, with increasing temperature, the steady state value of $\sigma_{\rm xz}$ decreases, but still one observes the stress-overshoot, albeit with a lesser value of $\sigma^{\rm max}$; see Fig. 1(b) for the corresponding data at $T = 0.4, 0.3, 0.2$ for an imposed $\dot{\gamma} = 10^{-4}$.

In Fig. 1(c), we illustrate the variation of $\sigma^{\rm max}$ with age, for a wide range of $\dot{\gamma}$ at $T = 0.2$. Thereafter, we demonstrate that at each temperature, the data for $\sigma^{\rm max}$ can be collapsed

onto a master curve using the relation

$$\sigma^{\max} = C(\dot{\gamma}, T) + A(T)\ln(\dot{\gamma} t_{\rm w}), \tag{2}$$

with $A(T)$ a temperature-dependent amplitude that is independent of $\dot{\gamma}$ and $t_{\rm w}$ and $C(\dot{\gamma}, T)$ a function that solely depends on $\dot{\gamma}$ and T.

Such a logarithmic relationship is motivated by Ree-Eyring's viscosity theory, modified appropriately to take into account the role of the sample's age, $t_{\rm w}$, as noted by Varnik et al.[5]. A similar dependence was also proposed by Rottler et al.[6] for the same binary LJ mixture subjected to uniaxial strain at a different state-point. Thus our scaling results are consistent with earlier observations. We note that such a logarithmic dependence is not observed in experiments involving other yield stress fluids like colloidal pastes[40] or carbopol[41] where a power-law increase is observed, which is also captured in the numerical simulations of model gels[42,43]. Thus, it seems that the response of dense thermal glasses are different from the low density materials with more complex structures.

Having observed the scale of the stress overshoot for various ages, imposed shear-rates and ambient temperatures, we will later explore whether such observations necessarily lead to the occurrence of transient shearbands.

2. Potential Energy

To have a measure of the structural changes in the system, both during the aging process and the onset of flow, we monitor the potential energy ($E_{\rm Pot}$) of the system. In Fig. 2(a), we show how the potential energy decreases when the system is quenched from the supercooled state at $T = 0.45$ to the lower temperatures $T = 0.2, 0.3, 0.4$. After the fast decrease during the initial aging regime, the potential energy decreases slowly, logarithmically depending on the age $t_{\rm w}$ of the system, as is typically observed during aging.

When the external shear is imposed on the system, the potential energy increases, with the steady state value depending upon the magnitude of the imposed shear-rate; see Fig. 2(b),(c) for $T = 0.2, 0.4$, respectively. Further, we check whether the potential energy of the system measured during the transient regime, prior to the onset of steady flow, is dependent on the initial age of the quiescent glass. As can be seen in Fig. 2(b), (c), for both the temperatures, the dependence on $t_{\rm w}$ becomes more visible with decreasing shear-rate. This thus indicates

that the system evolves through different intermediate structures, dependent on the initial state having different t_w, before steady states structures start getting explored. We now explore how these age-dependent transient structures are dynamically different. We also note that for the applied shear-rates, the approach to steady state seems faster for $T = 0.4$ than compared to $T = 0.2$. While in the former case, at long strain, the steady state potential energy, under applied shear, matches at large strains, this is not the case for $T = 0.2$. This combination of temperature, shear-rate and age of the sample will be further explored in later sections.

B. Single particle dynamics

1. Average MSD

In order to characterise the microscopic dynamical response of the glass, when yielding under shear, we monitor the single-particle dynamics. This is quantified by measuring the non-affine mean-squared displacement (MSD), Δr_z^2, in the direction transverse to the applied shear; the data is shown for $\dot{\gamma} = 10^{-4}$, at $T = 0.2$ (Fig. 3(a)) and $T = 0.4$ (in Fig. 3(c)). At both temperatures, during early times, particles exhibit ballistic motion, which is then followed by a caging regime. Subsequently, the onset of flow is marked by a super-linear regime, and eventually diffusive dynamics is observed. The onset of the super-linear or "super-diffusive" regime occurs around the stress overshoot in the stress-strain curve, when the stress, building up in the system, is released via the breaking of local cages leading to the subsequent diffusive motion of the particles[4,44]. We check how the initial age of the glassy state influences the measured Δr_z^2; the corresponding data is plotted in Fig. 3(a), (c) for the two temperatures. At both temperatures, both in the initial response and in the steady state, there is no visible difference in the measured MSD, for the samples having different ages. Only during the transient regime, where the onset of super-diffusive dynamics occurs, we observe variation with age of the quenched glass, with the effect more visible for $T = 0.4$; see Fig. 3(c). We also note that the onset timescale depends upon age, shifting to longer timescales with increasing t_w, as is clearly visible.

2. *Spatially resolved MSD*

To further probe the spatial features of the local dynamics during yielding, we divide the simulation box into eight layers of thickness $10\sigma_{\rm AA}$ along the z-direction. For each of these layers, we compute the averaged MSD for the particles populating it at $t = 0$, i.e. before shear is imposed. In Fig. 3(b), (d), we show the corresponding data, at $T = 0.2, 0.4$, respectively, for an imposed $\dot{\gamma} = 10^{-4}$ and age of $t_{\rm w} = 10^5$. We see that there is variation in the dynamics across the different layers, the variation being greater at $T = 0.2$ than at $T = 0.4$. While for $T = 0.4$, eventually, the long time dynamics seems to converge to the diffusive limit, within the timescale of observation, that is not the case for $T = 0.2$. In the latter case, while in one case, we see the onset of diffusive dynamics at long times, in some of the other slices, the dynamics continues to be sub-diffusive. To summarise, this demonstrates that, during yielding of the glass, at any temperature, dynamics is heterogeneous. However, the extent of heterogeneity and persistence increases with decreasing temperature. We will quantify that in more detail in the subsequent sections.

3. *MSD maps*

To visualise the dynamical heterogeneities, we construct three-dimensional maps of local MSD[16]. These maps are constructed in the following manner. We divide the simulation box into small cubic sub-boxes having linear size of $\sigma_{\rm AA}$. At any time t, we calculate the average MSD of the particles located in each sub-box at $t = 0$ (unsheared glassy state), which provides a cumulative picture of how yielding proceeds locally starting from the quiescent glass. As discussed earlier, we measure the z-component of MSD of each particle. The evolution of the three-dimensional maps with increasing strain, is shown in Fig. 4 and Fig. 5, for different ages of the glassy state at $T = 0.2$ and 0.4, respectively, corresponding to an imposed shear rate of $\dot{\gamma} = 10^{-4}$.

First, we focus on the situation at the lower temperature ($T = 0.2$); see Fig. 4. At early strain ($\dot{\gamma} = 0.1$), we observe localised "hot spots" of large mobilities[45,46]. At a strain of 0.5, more such local regions of faster dynamics have emerged. In the case of well aged initial state (e.g. $t_{\rm w} = 10^5$), we see that the hot spots are organised in the form of a shear band. On the other hand, for a younger initial state, i.e. $t_{\rm w} = 10^2$, these hot spots are

much more dispersed. At a later strain ($\dot{\gamma} = 1$), this difference is further amplified. For the younger sample, large regions of the system have been fluidized, whereas for the older system, enhanced mobility is still localised in the form of a shear band. Thus, the age of the initial glassy state, does influence the spatio-temporal organisation of regions of increased mobility. This is consistent with earlier findings in numerical simulations using different model systems[19] or predictions from theoretical models[29].

We now contrast this with the situation at the higher temperature ($T = 0.4$); see Fig. 5. At early strain ($\dot{\gamma} = 0.1$), we observe the hot spots, for all $t_{\rm w}$; however, there are more in number as compared to the case of $T = 0.2$, for any $t_{\rm w}$. With increased strain $\dot{\gamma} = 0.5$, we see that the hot spots have proliferated and cover almost the entire domain, including for the most aged sample. Thus, access to increased thermal fluctuations at higher temperatures lead to the tendency for a more homogenised and faster fluidisation of the glassy state under applied shear.

We will now carry out a more quantitative characterisation of this spatio-temporal response of the glassy states, sampled from different temperatures, and aged over different timescales.

4. Spatial profile of local mobility and fluctuations

So far, by spatially resolving the single particle MSDs, we demonstrated the existence of heterogeneous dynamics during yielding of the glass and how that depends on the temperature of the glassy state.

Using single particle MSDs, we construct the instantaneous spatial profile $\Delta r_z^2(z)/\langle \Delta r_z^2 \rangle$, which gives us a measure of fluctuations in local dynamics. The evolution of these profiles, with increasing strain, is shown in Fig. 6, for two different ages of the glass, viz. $t_{\rm w} = 10^2, 10^5$, under an imposed shear-rate of $\dot{\gamma} = 10^{-4}$, at $T = 0.2$. We observe that the spatial fluctuations are much larger and more persistent in the older sample, consistent with the qualitative discussion, above, involving MSD maps.

Using these spatial profiles, we can now quantify the contrast in local mobilities in the deforming glass, under applied shear, and compare the response across temperatures. In order to do that, we compute the fluctuations in local MSD, $\chi = (\Delta r_z^2(z) - \langle \Delta r_z^2 \rangle)^2 / \langle \Delta r_z^2 \rangle^2$ with increasing strain $\dot{\gamma}t$. Such a quantity measures the extent of fluctuations in average

mobilities, as characterised by the local MSD, across the regions parallel to the direction of flow. Defined in this manner, χ would therefore easily capture the contrast in the dynamics during the formation of shear-bands. To note, such a quantity is different from the dynamical susceptibility, χ_4, which is a measure of fluctuations in single particle dynamics, measured within the steady-state ensemble. Here, we are concerned with the fluctuations across regions during the onset of flow from a quiescent state.

The corresponding data, for temperatures $T = 0.2, 0.3, 0.4$, across ages $t_{\rm w} = 10^2, 10^3, 10^4, 10^5$, for a range of imposed shear-rates, viz. $\dot{\gamma} = 10^{-2}, 10^{-3}, 10^{-4}$, are shown in Fig. 7. Typically, χ behaves non-monotonically with increasing strain, with the maximal spatial fluctuations ($\chi^{\rm max}$) occuring at a strain which corresponds to the super-linear regime in the MSD (see Fig. 3); i.e., once yielding of the glass has occurred. Further, for a fixed $\dot{\gamma}$, the magnitude of $\chi^{\rm max}$ increases with age, i.e. the contrast in mobilities across a sample becomes largest for a more aged sample. Importantly, we also note that $\chi^{\rm max}$ also starts increasing when we shear the glasses with smaller and smaller shear-rates; e.g. see Fig. 7(a)-(c), for the variation of $\chi^{\rm max}$ with age and imposed shear-rate. With decreasing temperature, this spatial fluctuation increases even further.

To get a more complete picture of the variation of these spatial fluctuations, across age and temperature, we plot the corresponding contour maps for $\chi(t_{\rm w}, \dot{\gamma})$; these are shown in Fig. 8. From the contour maps, one can infer how strong and persistent the spatial fluctuations are with varying temperature, age and imposed shear-rate. It is evident that for large shear-rates ($\dot{\gamma} = 10^{-2}$), these fluctuations are negligible at any age of the glassy state sampled at any of the temperatures; see Fig. 8(a),(d),(h). On the other hand, at smaller shear-rates ($\dot{\gamma} = 10^{-4}$), large fluctuations are visible at all temperatures. However, the age of the sample then becomes a factor in determining the degree of fluctuations and persistence with increasing strain. At a lower temperature, $T = 0.2$, these are prominent over the range of ages we investigated and also persistent over large strains; see Fig. 8(i). On the other hand, at higher temperatures, $T = 0.4$ (Fig. 8(c)), that scale of fluctuations is only slightly visible at very large ages over a small strain window. The range of ages and strain-interval over which similar fluctuations are seen broadens out at an intermediate temperature of $T = 0.3$ (Fig. 8(f)) and, even more extensively, at $T = 0.2$. This trend is also evident at an intermediate shear-rate of $\dot{\gamma} = 10^{-3}$, with the scale of fluctuations being less but visible (Fig. 8(h)); howevever, it is important to note that the fluctuations are nearly negligible at

the higher temperature $T = 0.4$ at this shear-rate (Fig. 8(b)). Thus, we demonstrate, that the scale of transient dynamical heterogeneities depend on a combination of temperature of the glass, its age and the imposed shear-rate. Since the quantity we compute, $\chi(t_{\rm w}, \dot{\gamma})$, measures the contrast in mobilities in layers parallel to the flow direction, the conclusions drawn from the contour maps allow us to infer that the propensity to shear-band during yielding is determined on how rigid the glass is and how small/large the applied shear-rate is.

5. Time evolution of shear-bands

Finally, we study how a transient shear-band, once formed, spatially evolves with time. Such analysis can only be done for the case where a well-defined shear-band can be identified. Thus, we focus at the case of $T = 0.2$ and small shear-rate ($\dot{\gamma} = 10^{-4}$), where we observe transient shear-bands for a range of $t_{\rm w}$.

In order to further quantify and characterise the spatio-temporal evolution of the shear-band, we define a region to be mobile or not, by setting a threshold $\mu_{th} = 0.02$ on the local Δr_z^2. As can be seen in Fig. 3(a), such a choice of μ_{th} is larger than the plateau value in the MSD and thus corresponds to motions beyond cage-breaking. We then define the local mobility ψ as

$$\psi = \begin{cases} 1 & \text{if } \mu \geq \mu_{th}, \\ 0 & \text{otherwise,} \end{cases} \tag{3}$$

where μ is the average MSD of particles in a sub-box. Following this convention, we digitize the whole system into mobile and immobile regions. An example of the mobility map, thus constructed, is shown in Fig. 9(a).

We quantify the extent of fluidisation in the system by measuring the fraction of mobile cells, p, at any given instant. The evolution of p as a function of strain, for an imposed shear of $\dot{\gamma} = 10^{-4}$, is shown in Fig. 9(b). We observe that independent of age ($t_{\rm w}$), the sudden initial increase of p occurs nearly at the same strain. However, the subsequent increase in p does depend upon the age and thus, the fraction of system which is mobilised at $\dot{\gamma}t = 0.2$ is substantially larger for $t_{\rm w} = 10^2$ as compared to $t_{\rm w} = 10^5$.

Further, we try to identify the spatial organisation of these mobile cells. By locating contiguous layers of mobile cells, we identify the formation of the shear band and, thereafter,

by marking the interfaces of this band, we measure how the band-width, $\xi_{\rm b}$, evolves with time. For different ages of the initial glassy state, this time evolution is shown in Fig. 9(c), for a fixed $\dot{\gamma} = 10^{-4}$. We see that $\xi_{\rm b}$ initially grows quickly and then eventually it reaches a regime where the data can be fitted with $\xi_{\rm b} \sim t^{1/2}$, implying that the propagating interface of the shear band has a diffusive motion. This diffusive regime is not extensively dependent on $t_{\rm w}$, although samples having largest $t_{\rm w}$ do seem to display a slower motion of the spreading interface.

IV. SUMMARY AND CONCLUSIONS

To summarize, we have used numerical simulations of a model glass former, to probe the mechanical response of amorphous solids, having different aging histories, by imposing a wide range of external shear rates. The response is studied at different temperatures below the mode coupling temperature, in order to ascertain how thermal fluctuations affect the spatio-temporal response. We underline, here, that the numerical simulations are done by integrating the Newton's equations of motions using Lees-Edwards periodic boundary conditions and the local DPD thermostat. This, thus, allows for unhindered spatio-temporal fluctuations as the glassy state responds to the applied shear, without introducing any biases or suppressing any fluctuations, which would be the case if one were using walls[15] or integrating the SLLOD equations along with some global thermostat (like Nose-Hoover)[33]. Therefore, qualitatively, the nature of dynamical heterogeneities observed could be different from the earlier works.

The macroscopic response of the glass is characterized by the occurrence of a overshoot in the stress-strain curves, observed for the range of shear-rates and ages that we have studied, at the different temperatures. Consistent with earlier works, we find that, at each temperature, the peak height can be scaled on to a master-curve as a function of $\dot{\gamma} t_{\rm w}$. The corresponding potential energies of the system, measured during the deformation process, show a dependence on age with decreasing shear rate. This implies that the structures visited during the transient regime, prior to the onset of steady flow, start becoming different, depending upon the initial history. We also observe that for lower temperatures, it takes longer for potential energies to reach the steady state value at smaller shear-rates, reflecting the role of thermal fluctuations in affecting the duration of the transient regime for these

parameters.

This is further revealed, by measuring dynamical quantities at the microscopic scale. Our probe of choice is the time evolution of non-affine mean squared displacement (MSD) of the particles relative to the initial quiescent state. Spatial profiles of the MSD show that for a fixed imposed shear and age, the transient dynamics is more heterogeneous and more long-lived at lower temperatures. This is illustrated by constucting sptatially resolved three-dimensional maps which provide a handle to visualize the extent of dynamical heterogeneity as the glassy states respond to the imposed shear. Such maps demonstrate that the heterogeneities are spatially localised in the form of shearbands, for old enough systems at low temperatures.

We quantify the extent of dynamical heterogeneity organised in the form of shear-bands, by measuring the degree of fluctuations, χ, in local mobilities across regions oriented parallel to the direction of imposed flow. Thus, large values in χ reflect more propensity of the system to exhibit shear-banding. We do such measurements by scanning across entire range of shear-rates and thermal histories explored by us. We observe that the fluctuations are maximum around the yielding strain and the peak in fluctuations increase with decreasing shear-rate as well as larger ages. Further by constructing contour maps of $\chi(t_{\rm w}, \dot{\gamma}t)$ for varying shear-rates at different temperatures, we demonstrate that the emergence of significant shear-banding depends upon the combination of temperature, age and imposed shear-rate. The contrast in local mobilites is most prominent at low shear-rates and low temperatures, where the age of the system does not seem to matter, over the range explored by us. With increasing temperature, the age of the sample starts to determine whether transient shear-banding will be visible or not. For even higher temperatures, one has to go to lower shear-rates and even older systems in order for such largely localized heteroegeneities to be visible. Also, in the cases where shear-bands can be identified, we observe that the spreading of the shear-band across the system seems to depend on age, albeit weakly.

Thus, our study shows that the transient shearbanding, with sharply contrasting mobilities across regions, only occur for specific combinations of temperature, shear-rate and age, as discussed above. Note that, for most of the glassy samples that we study, the macroscopic response under an imposed strain-rate is characterized by the stress overshoot. Yet, the transient shear-bands are only visible in only a subset of the cases we study. Thus, the occurrence of a stress overshoot does not necessarily lead to the transient shearbands,

quantified via the mobilities relative to the initial quiescent state, as predicted by the spatially resolved fluidity and SGR models[10,29,30]. On the other hand, as predicted by these and other models[31,32,34,35], we do observe that the propensity to shearband is more in the case of increasingly aged samples. However, the choice of disorder distributions in these models (e.g. distribution of yielding thresholds), with changing age, remains arbitrary, and it would be useful to obtain these as inputs from atomistic simulations.

The transient shear-banding observed in our numerical simulations as well as other, bears resemblance to dynamical heterogeneities observed in thermal glasses[47], except that in the case of a sheared glass, strong anisotropies come into play leading to the spatial localisation. In the case of supercooled liquids, the scale of dynamical heterogeneities increases as the temperature is decreased towards the putative glass transition temperature. Similarly, in the case of applied shear, the heterogeneous dynamics is enhanced as one approaches vanishingly small shear-rates, with the yield stress being identified as a critical threshold[27,48,49]. Also, it is possible that the regime of imposed shear-rates over which the critical threshold influences flow[21,50] could change with temperature, with decreasing thermal fluctuations extending this regime over longer scales. This would rationalise why with increasing temperatures, the contrast in heterogeneities progressively decreases, for a fixed shear-rate. Over and above, the aging effects are more prominent at higher temperatures, with the glass remembering the history from where it was quenched over longer aging timescales[47,50]. At low temperature, thus, structural arrest and therefore rigidity emerges at shorter timescale. Hence, the mechanical response of the glass, having the same age and same imposed shear-rate, would be different across temperatures. This interplay of different timescales therefore brings about the complex response as a function of all these control parameters. Eventually, it would be useful to quantify the exact ranges in these control parameters, where we expect transient but prominent shearbanding to be visible.

The transient dynamical heterogeneities that we track and analyse are similar to measurements done via confocal microscopy in colloidal glasses[11] or scattering measurements in granular systems[45]. This is different from using velocity profiles as a diagnostic tool, which capture plasticity over short timescales. Further, in our case, because of periodic boundary conditions, the shear bands can emerge anywhere in the system, unlike many cases where initial mobile regions happen to occur near confining surfaces[11,41]. However, similar to experiments, we do observe the propagation of the mobile front to eventually fluidize the system.

Acknowledgement:

We achnowledge financial support by the Deutsche Forschungsgemeinschaft (DFG) in the framework of the priority programme SPP 1594 (Grant No. HO 2231/8-2). PC thanks FOR 1394 for financial support during visit to University of Düsseldorf.

REFERENCES

[1]Binder, K. and Kob, W., *Glassy Materials and Disordered Solids: An Introduction to Their Statistical Mechanics*, (World Scientific, Singapore, 2011).

[2]Rodney, D., Tanguy, A., and Vandembroucq, D., Modeling the mechanics of amorphous solids at different length scale and time scale, *Modelling Simul. Mater. Sci. Eng.* **19**, 083001 (2011).

[3]Barrat, J.-L. and Lemaitre, A. Dynamical Heterogeneities in Glasses, Colloids, and Granular Materials, Chap. 8, edited by L. Berthier, G. Biroli, J.-P. Bouchaud, L. Cipelletti, and W. van Saarloos (Oxford University Press, Oxford, 2011).

[4]Zausch, J., Horbach, J., Laurati, M., Egelhaaf, S. U., Brader, J. M., Voigtmann, T., and Fuchs, M., From Equilibrium to Steady State: The Transient Dynamics of Colloidal Liquids under Shear, *J. Phys.: Condens. Matter* **20**, 404210 (2008).

[5]Varnik, F., Bocquet, L., and Barrat, J.-L., A study of the static yield stress in a binary Lennard-Jones glass, *J. Chem. Phys.* **120**, 2788 (2004).

[6]Rottler, J. and Robbins, M. O., Unified Description of Aging Rate Effects in Yield of Glassy Solids, *Phys. Rev. Lett.* **95**, 225504 (2005).

[7]Schuh, C. A., Hufnagel, T. C., and Ramamurty, U., Mechanical behavior of amorphous alloys, *Acta Mater.* **55**, 4067 (2007).

[8]Møller, P. C. F., Rodts, S., Michels, M. A. J., and Bonn, D., Shear banding and yield stress in soft glassy materials, *Phys. Rev. E* **77**, 041507 (2008).

[9]Divoux, T., Fardin, M. A., Manneville, S., and Lerouge, S., Shear Banding of Complex Fluids, *Ann. Rev. of Fluid Mech.*, **48**, 81 (2016).

[10]Fielding, S. M., Shear banding in soft glassy materials, *Rep. Prog. Phys.* **77**, 102601 (2014).

[11]Chikkadi, V., Wegdam, G., Bonn, D., Nienhuis, B., and Schall, P., Long-Range Strain Correlations in Sheared Colloidal Glasses. *Phys. Rev. Lett.* **107**, 198303 (2011).

[12]Besseling, R., Isa, L., Ballesta, P., Petekidis, G., Cates, M. E., and Poon, W. C. K., Shear Banding and Flow-Concentration Coupling in Colloidal Glasses, *Phys. Rev. Lett.* **105**, 268301 (2010).

[13]Bokeloh, J., Divinski, S. V., Reglitz, G., and Wilde, G., Tracer Measurements of Atomic Diffusion inside Shear Bands of a Bulk Metallic Glass, *Phys. Rev. Lett.* **107**, 235503 (2011).

[14]Divoux, T., Tamarii, D., Barentin, C., and Manneville, S., Transient Shear Banding in a Simple Yield Stress Fluid. *Phys. Rev. Lett.* **104**, 208301 (2010).

[15]Varnik, F., Bocquet, L., Barrat, J.-L., and Berthier, L., Shear Localization in a Model Glass. *Phys. Rev. Lett.* **90**, 095702 (2003).

[16]Chaudhuri, P. and Horbach, J., Onset of flow in a confined colloidal glass under an imposed shear stress, *Phys. Rev. E* **88**, 040301(R) (2013).

[17]Irani, E., Chaudhuri, P., and Heussinger, C., Impact of attractive interactions on the rheology of dense athermal particles, *Phys. Rev. Lett.* **112**, 188303 (2014).

[18]Shrivastav, G. P., Chaudhuri, P., and Horbach, J., Formation and growth of shear bands in glasses: existence of an underlying, directed percolation transition, preprint arXiv:1506.03049.

[19]Shi, Y. and Falk, M. L., Atomic-scale simulations of strain localization in three-dimensional model amorphous solids, *Phys. Rev. B* **73**, 214201 (2006).

[20]Bailey, N. P., Schiotz, J., and Jacobsen, K. W., Atomistic simulation study of the shear-band deformation mechanism in Mg-Cu metallic glasses, *Phys. Rev. B* **73**, 064108 (2006).

[21]Chaudhuri, P., Berthier, L., and Bocquet, L., Inhomogeneous shear flows in soft jammed materials with tunable attractive forces, *Phys. Rev. E* **85** 021503 (2012).

[22]Dasgupta, R., Hentschel, H. G. E., and Procaccia, I., Microscopic Mechanism of Shear Bands in Amorphous Solids, *Phys. Rev. Lett.* **109** 255502 (2012).

[23]Nordstrom, K. N., Verneuil, E., Arratia, P. E., Basu, A., Zhang, Z., Yodh, A. G., Gollub, J. P., and Durian, D. J., Microfluidic Rheology of Soft Colloids above and below Jamming, *Phys. Rev. Lett.* **105**, 175701 (2010).

[24]Bonn, D., Paredes, J., Denn, M. M., Berthier, L., Divoux, T. and Manneville, S., Yield stress materials in soft condensed matter, preprint arXiv:1502.0528.

[25]Martens, K., Bocquet, L., and Barrat, J.-L., Spontaneous formation of permanent shear bands in a mesoscopic model of flowing disordered matter, *Soft Matter* **8**, 4197 (2012).

[26]Coussot, P. and Ovarlez, G., Physical origin of shear-banding in jammed systems, *Eur.*

Phys. J. E **33**, 183 (2010).

[27]Divoux, T., Tamarii, D., Barentin, C., Teitel, S. and Manneville, S., Yielding dynamics of a Herschel-Bulkley fluid: a critical-like fluidization behaviour, *Soft Matter* **8**, 4151 (2012).

[28]Tsamados, M., Plasticity and dynamical heterogeneity in driven glassy materials, *Euro. Phys. J. E* **32**, 165 (2010).

[29]Moorcroft, R. L., Cates, M. E., and Fielding, S. M., Age-Dependent Transient Shear Banding in Soft Glasses, *Phys. Rev. Lett.* **106**, 055502 (2011).

[30]Moorcroft, R. L. and Fielding, S. M., Criteria for Shear Banding in Time-Dependent Flows of Complex Fluids. *Phys. Rev. Lett.* **110**, 086001 (2013).

[31]Manning, M. L., Langer, J. S. and Carlson, J. M., Strain localization in a shear transformation zone model for amorphous solids, *Phys. Rev. E* **76**, 056106 (2007).

[32]Manning, M. L., Daub, E. G., Langer, J. S. and Carlson, J. M., Rate-dependent shear bands in a shear-transformation-zone model of amorphous solids, *Phys. Rev. E* **79**, 016110 (2009).

[33]Shi, Y., Katz, M. B., Li, H. and Falk, M. L., Evaluation of the Disorder Temperature and Free-Volume Formalisms via Simulations of Shear Banding in Amorphous Solids, *Phys. Rev. Lett.* **98**, 185505 (2007).

[34]Jagla E. A., Shear band dynamics from a mesoscopic modeling of plasticity, *J. Stat. Mech.* P12025 (2010).

[35]Vandembroucq, D. and Roux, S., Mechanical noise dependent aging and shear banding behavior of a mesoscopic model of amorphous plasticity, *Phys. Rev. B* **84**, 134210 (2011).

[36]Kob, W. and Andersen, H. C., Scaling Behavior in the β-Relaxation Regime of a Supercooled Lennard-Jones Mixture, *Phys. Rev. Lett.* **73**, 1376 (1994).

[37]Plimpton, S., Fast Parallel Algorithms for Short-Range Molecular Dynamics, *J. Comp. Phys.* **117**, 1 (1995).

[38]Soddemann, T., Dünweg, B., and Kremer, K., Dissipative particle dynamics: A useful thermostat for equilibrium and nonequilibrium molecular dynamics simulations, *Phys. Rev. E* **68**, 046702 (2003).

[39]Lees, A. W. and Edwards, S. F., The computer study of transport processes under extreme conditions, *J. Phys. C: Solid State Phys.* **5**, 1921 (1972).

[40]Derec, C., Ducouret, G., Ajdari, A. and Lequeux, F., Aging and nonlinear rheology in suspensions of polyethylene oxideprotected silica particles, *Phys. Rev. E* **67**, 061403 (2003).

[41]Divoux, T., Barentin, C. and Manneville, S., Stress overshoot in a simple yield stress fluid: An extensive study combining rheology and velocimetry, *Soft Matter*, **7**, 9335 (2011).

[42]Park, J. D. and Ahn, K. H., Structural evolution of colloidal gels at intermediate volume fraction under start-up of shear flow, *Soft Matter* **9**, 11650 (2013).

[43]Whittle, M. and Dickinson, E., Stress overshoot in a model particle gel, *J. Chem. Phys.* **107**, 10191 (1997)

[44]Koumakis, N., Laurati, M., Egelhaaf, S.U., Brady, J.F, and Petekidis, G., Yielding of Hard-Sphere Glasses during Start-Up Shear, *Phys. Rev. Lett.* **108**, 098303 (201).

[45]Amon, A., Bruand, A., Crassous, J., and Clément, J., Hot spots in an athermal system, *Phys. Rev. Lett.* **108**, 135502 (2012).

[46]Sentjabrskaja, T., Chaudhuri, P., Hermes, M., Poon, W. C. K., Horbach, J., Egelhaaf, S. U., and Laurati, M., Microscopic dynamics during creep in colloidal glasses, *Sci. Rep.* **5**, 11884 (2015).

[47]Berthier, L., and Biroli, G., Theoretical perspective on the glass transition and amorphous materials, *Rev. Mod.* Phys. **83**, 587 (2011).

[48]Bocquet, L., Colin, A., Ajdari, A., Kinetic Theory of Plastic Flow in Soft Glassy Materials *Phys. Rev. Lett.* **103**, 036001 (2009).

[49]Liu, C., Ferrero, E. E., Puosi, F., Barrat, J.-L., Martens, K., Driving Rate Dependence of Avalanche Statistics and Shapes at the Yielding Transition, *Phys. Rev. Lett.* **116**, 065501 (2016).

[50]Berthier, L., Yield stress, heterogeneities and activated processes in soft glassy materials, *J. Phys. Cond. Matt.* **15**, S933 (2003).

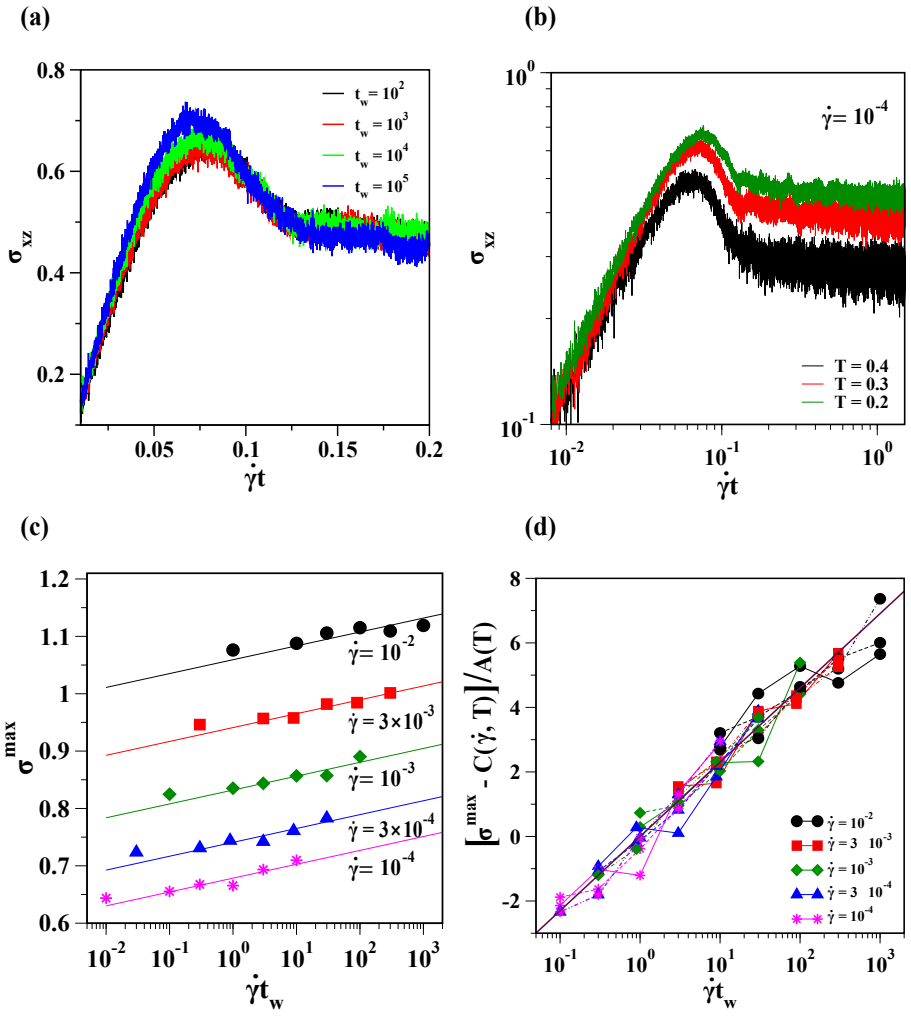

FIG. 1. (a) Evolution of macroscopic stress, $\sigma_{\rm xz}$ with increasing strain, under an imposed $\dot{\gamma} = 10^{-4}$ during yielding, for initial glassy states having different ages $t_{\rm w}$, at $T = 0.2$. (b) For a fixed shear-rate ($\dot{\gamma} = 10^{-4}$) and age ($t_{\rm w} = 10^4$), evolution of $\sigma_{\rm xz}$ with strain at different temperatures, $T = 0.2, 0.3, 0.4$. (c) The variation of peak height of stress overshoot, $\sigma^{\rm max}$, with age $t_{\rm w}$, for different imposed $\dot{\gamma}$ at $T = 0.2$. Solid lines show the fitting of data with a logarithmic fitting function, $\sigma^{max} = C_1(\dot{\gamma}) + A_1 \ln(\dot{\gamma}t)$. (d) Scaling of $\sigma^{\rm max}$ with $\ln(\dot{\gamma}t_{\rm w})$ at $T = 0.2, 0.3, 0.4$.

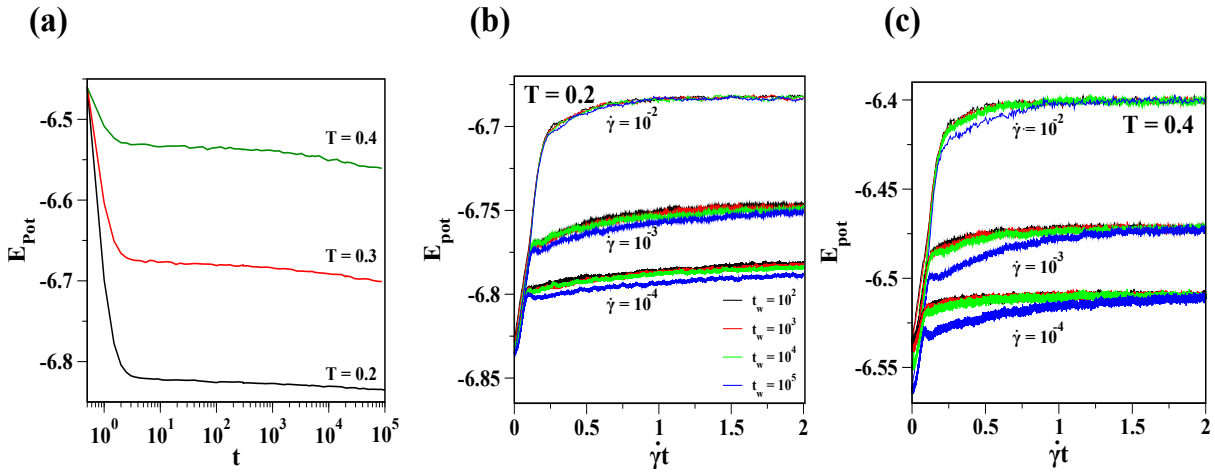

FIG. 2. (a) Evolution of potential energy ($E_{\rm Pot}$) of the quiescent glass during aging for three different temperatures, showing typical logarithmic decay. (b) For $\dot{\gamma} = 10^{-2}, 10^{-3}, 10^{-4}$, increase of potential energy with strain ($\dot{\gamma}t$) for different $t_{\rm w}$ of the quiescent glass at $T = 0.2$. (c) Similar plot as in (b) for T=0.4

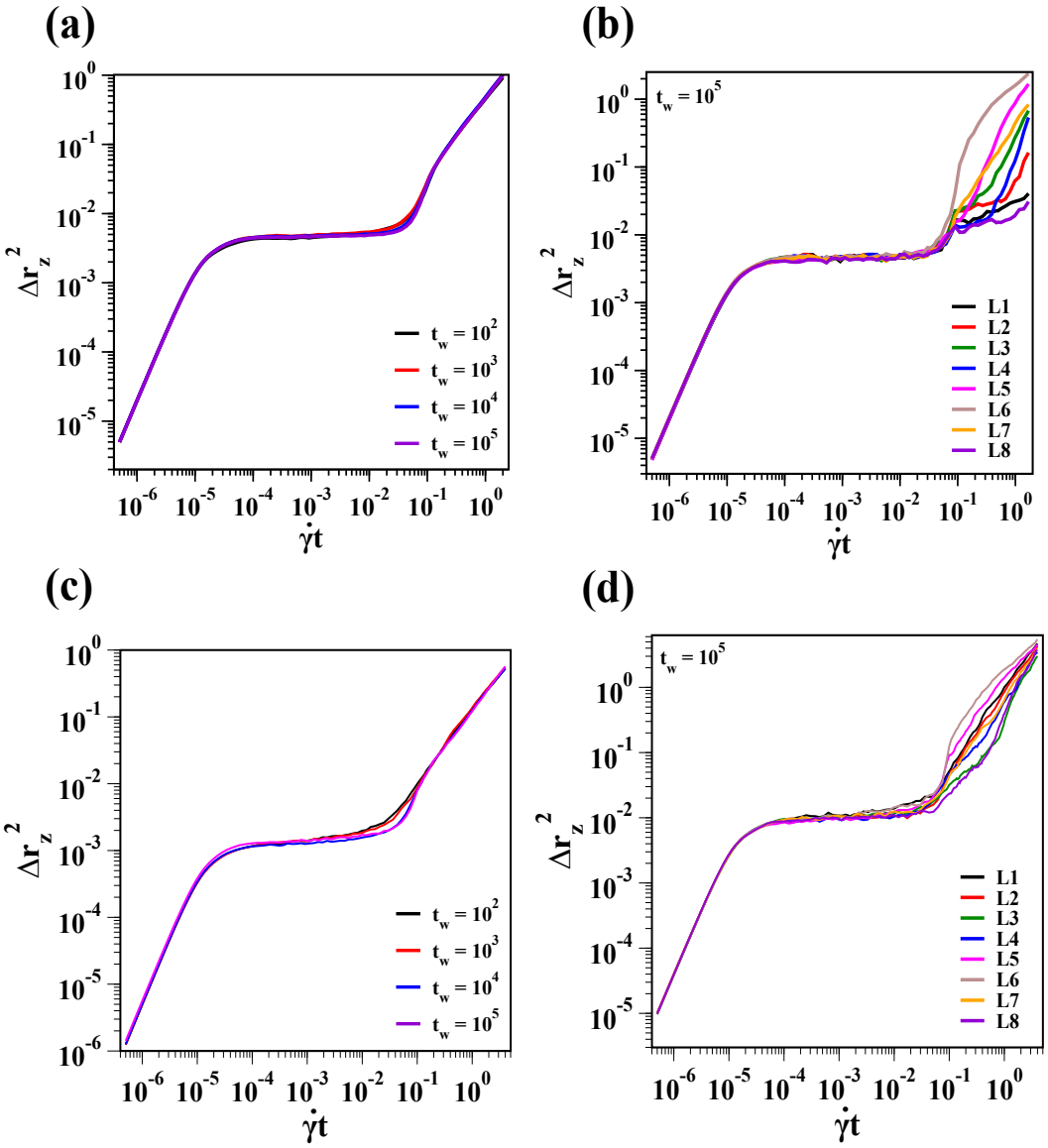

FIG. 3. (Top) $T = 0.2$: (a) Variation in z-component single particle MSD, Δr_z^2, with age for a fixed imposed $\dot{\gamma} = 10^{-4}$. (b) Spatial variation in MSD for $\dot{\gamma} = 10^{-4}$ and $t_{\rm w} = 10^5$. (Bottom) $T = 0.4$ (c) Variation in Δr_z^2, with $t_{\rm w}$ for imposed $\dot{\gamma} = 10^{-4}$. (d) Spatial variation in MSD for $\dot{\gamma} = 10^{-4}$ and $t_{\rm w} = 10^5$.

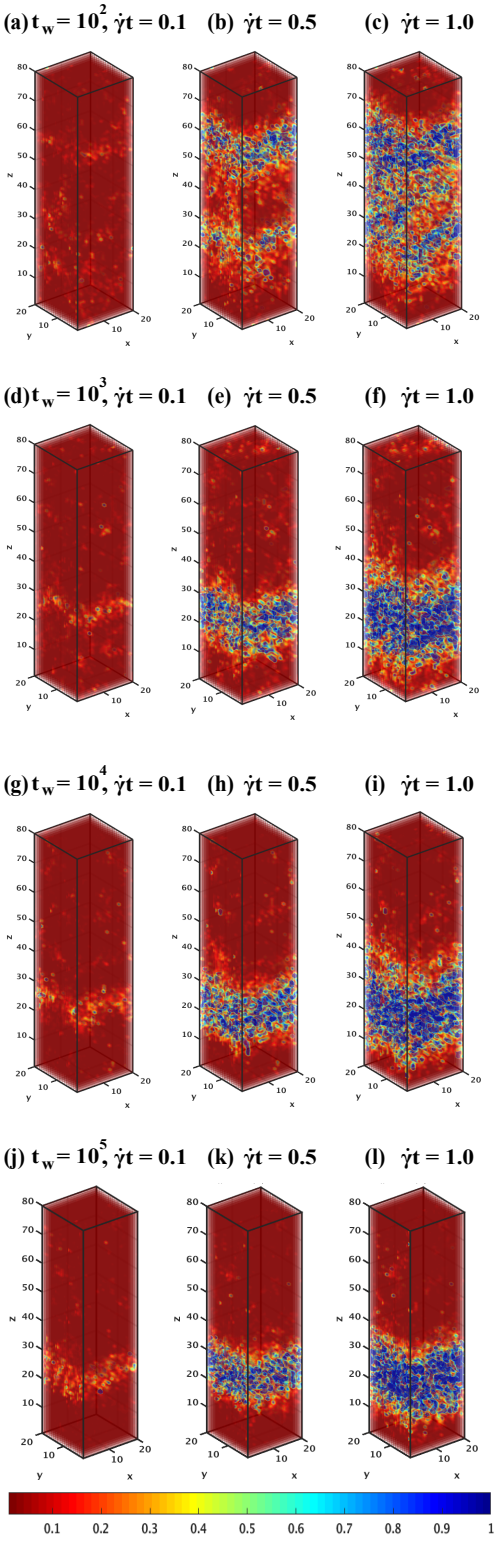
(a) $t_w = 10^2$, $\dot{\gamma}t = 0.1$
(b) $\dot{\gamma}t = 0.5$
(c) $\dot{\gamma}t = 1.0$
(d) $t_w = 10^3$, $\dot{\gamma}t = 0.1$
(e) $\dot{\gamma}t = 0.5$
(f) $\dot{\gamma}t = 1.0$
(g) $t_w = 10^4$, $\dot{\gamma}t = 0.1$
(h) $\dot{\gamma}t = 0.5$
(i) $\dot{\gamma}t = 1.0$
(j) $t_w = 10^5$, $\dot{\gamma}t = 0.1$
(k) $\dot{\gamma}t = 0.5$
(l) $\dot{\gamma}t = 1.0$
0.1 0.2 0.3 0.4 0.5 0.6 0.7 0.8 0.9 1

FIG. 4. At $T = 0.2$, for imposed shear rate of $\dot{\gamma} = 10^{-4}$, MSD maps at different strains, during the yielding of the glass of different ages $t_w = 10^2(\text{top}), t_w = 10^3(\text{second}), t_\text{w} = 10^4(\text{third}), t_\text{w} = 10^5(\text{bottom})$.

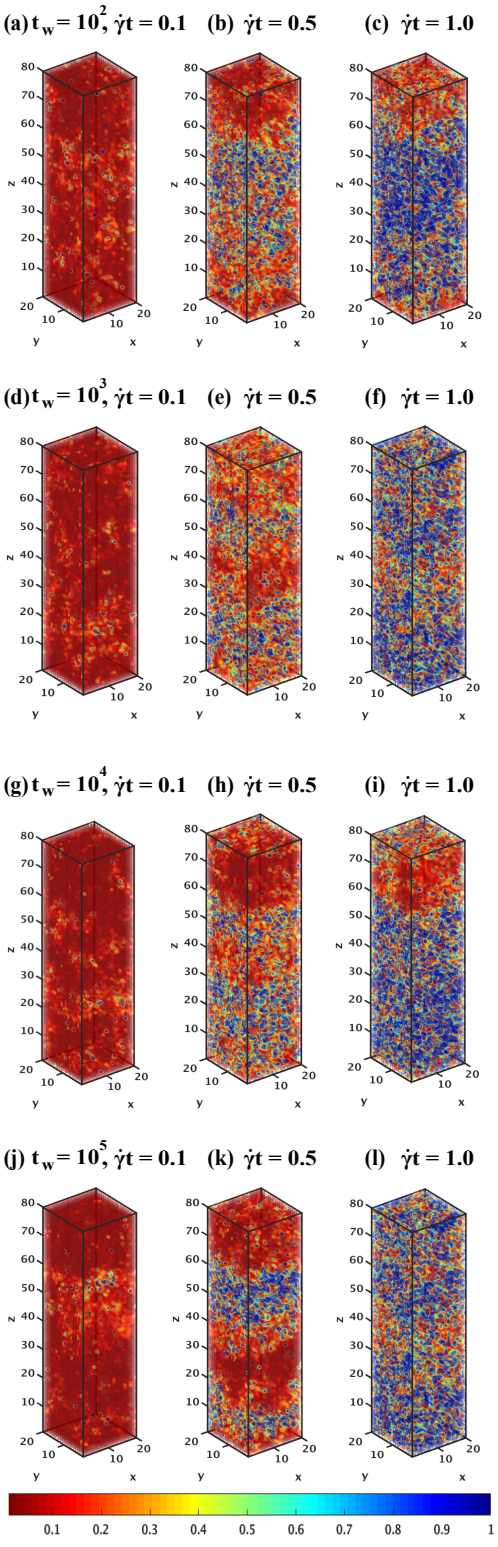
(a) $t_w = 10^2$, $\dot{\gamma}t = 0.1$
(b) $\dot{\gamma}t = 0.5$
(c) $\dot{\gamma}t = 1.0$
(d) $t_w = 10^3$, $\dot{\gamma}t = 0.1$
(e) $\dot{\gamma}t = 0.5$
(f) $\dot{\gamma}t = 1.0$
(g) $t_w = 10^4$, $\dot{\gamma}t = 0.1$
(h) $\dot{\gamma}t = 0.5$
(i) $\dot{\gamma}t = 1.0$
(j) $t_w = 10^5$, $\dot{\gamma}t = 0.1$
(k) $\dot{\gamma}t = 0.5$
(l) $\dot{\gamma}t = 1.0$
z
y
x
0.1 0.2 0.3 0.4 0.5 0.6 0.7 0.8 0.9 1

FIG. 5. At $T = 0.4$, for imposed shear rate of $\dot{\gamma} = 10^{-4}$, MSD maps at different strains, during the yielding of the glass of different ages $t_{\rm w} = 10^2$(top), $t_{\rm w} = 10^3$(second), $t_{rmw} = 10^4$(third), $t_{\rm w} = 10^5$(bottom).

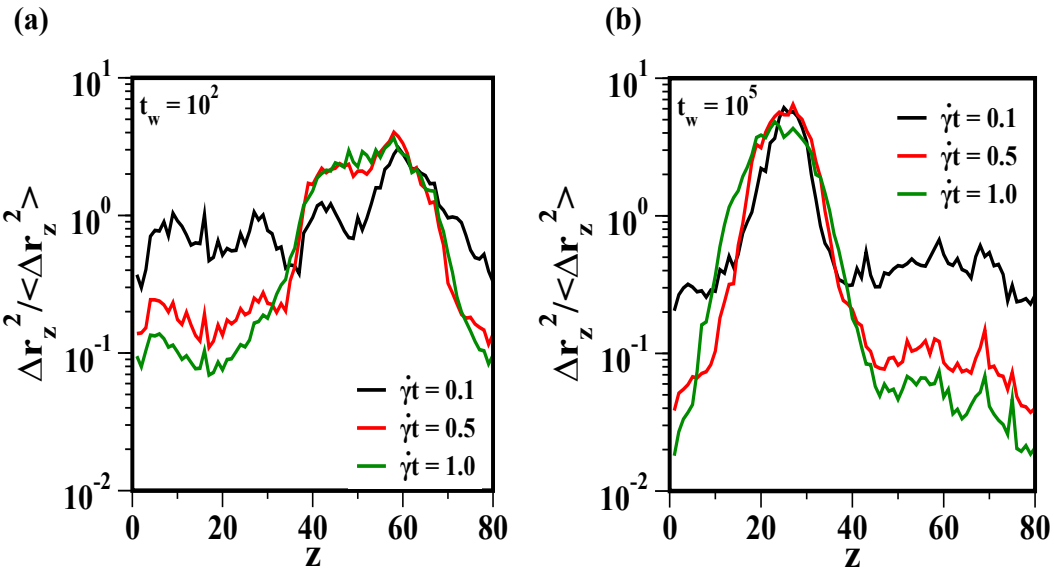

FIG. 6. Evolution of spatial profiles of local MSD, $\Delta r_z^2(z)/\langle\Delta r_z^2\rangle$, with strain for (a) $t_w = 10^2$, (b) $t_w = 10^5$, under an imposed shear of $\dot{\gamma} = 10^{-4}$.

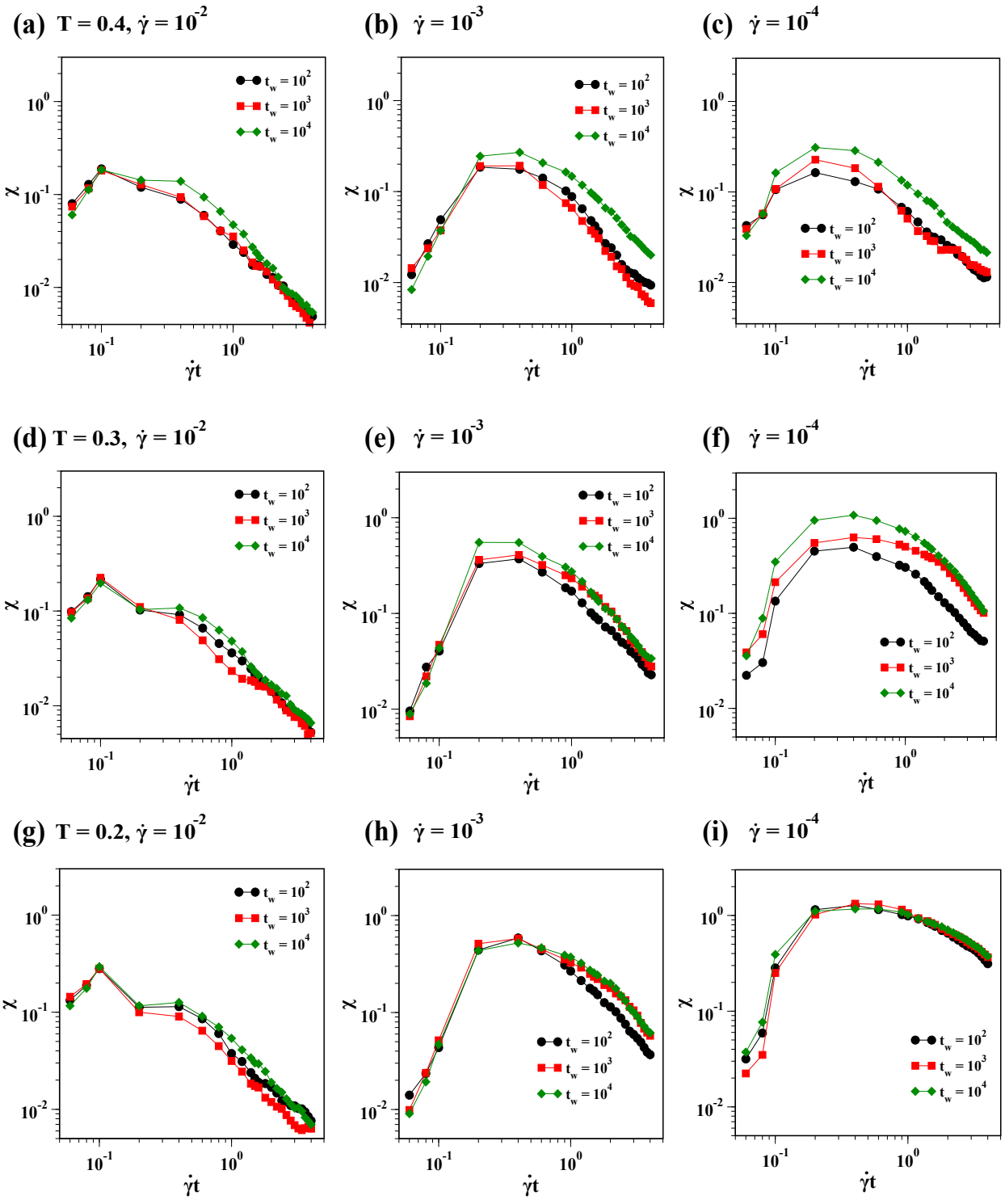
(a) T = 0.4, $\dot{\gamma} = 10^{-2}$
(b) $\dot{\gamma} = 10^{-3}$
(c) $\dot{\gamma} = 10^{-4}$
(d) T = 0.3, $\dot{\gamma} = 10^{-2}$
(e) $\dot{\gamma} = 10^{-3}$
(f) $\dot{\gamma} = 10^{-4}$
(g) T = 0.2, $\dot{\gamma} = 10^{-2}$
(h) $\dot{\gamma} = 10^{-3}$
(i) $\dot{\gamma} = 10^{-4}$
$t_w = 10^2$
$t_w = 10^3$
$t_w = 10^4$
χ
$\dot{\gamma}t$

FIG. 7. Variation of the fluctuations in local MSD, χ, with strain for different $t_{\rm w}$, at $\dot{\gamma} = 10^{-2}$, 10^{-3}, 10^{-4} (left to right), for glassy states sampled at temperatures $T = 0.4$ (top row), 0.3 (middle row), 0.2 (bottom row).

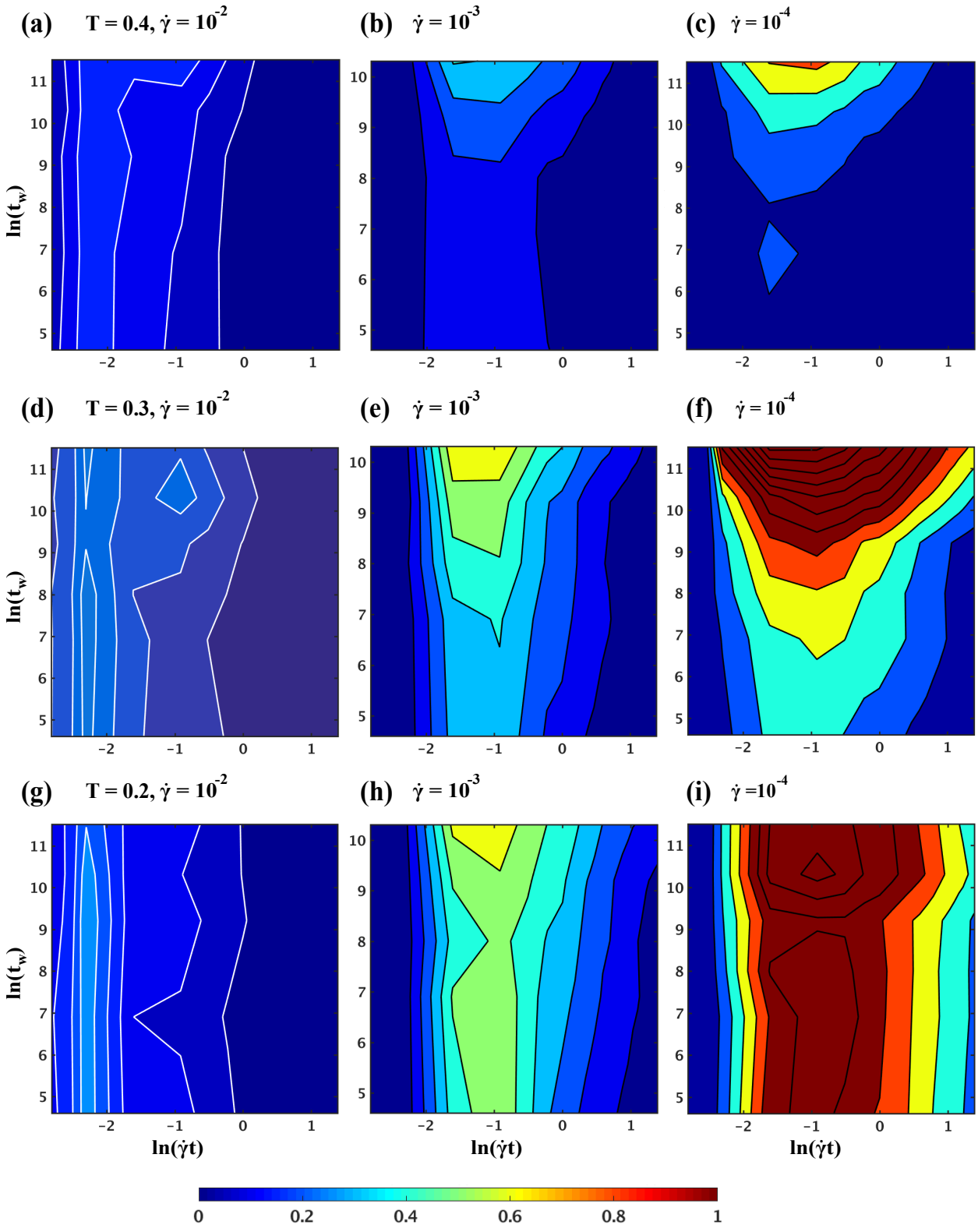

FIG. 8. Contour maps of $\chi(t_{\rm w}, \dot{\gamma}t)$, for $T = 0.4$ (top panel), $T = 0.3$ (middle panel), $T = 0.2$ (bottom panel), under imposed shear-rates of $\dot{\gamma} = 10^{-2}, 10^{-3}, 10^{-4}$ (from left to right in each panel).

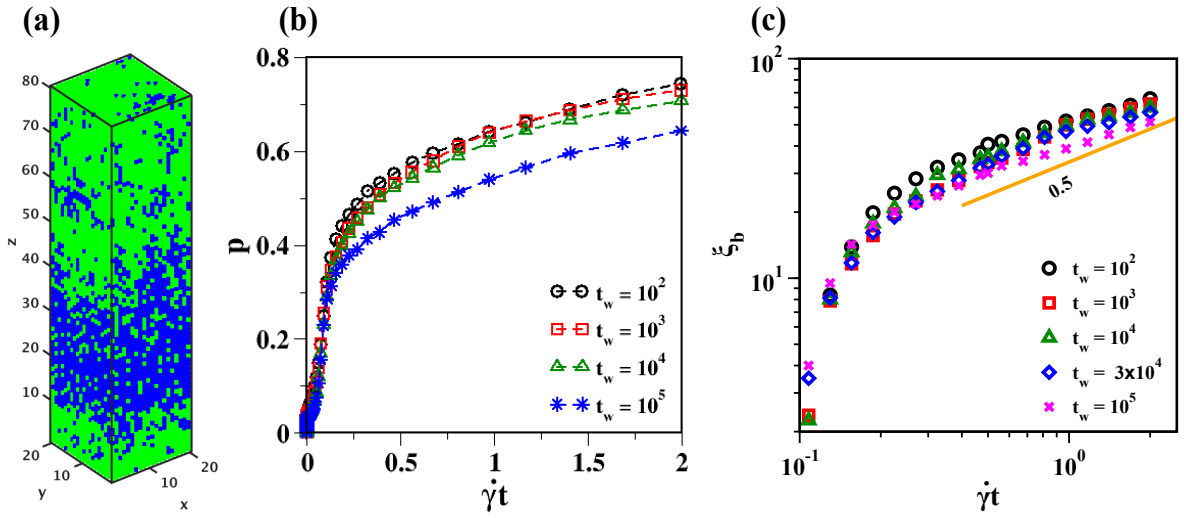

FIG. 9. (a) Map of local mobility ψ of a sample of an age $t_{\rm w} = 10^4$ for $T = 0.2$, $\dot{\gamma}t = 0.5$. Mobile regions are marked in blue while immobile regions are marked in green. (b) Growth of fraction of mobile regions with increasing strain, for imposed $\dot{\gamma} = 10^{-4}$ and different ages. (c) Increasing width of the shearband, ξ_b, with strain for different $t_{\rm w}$, at imposed $\dot{\gamma} = 10^{-4}$.